Quantum Information Processing with Nanomechanical Qubits

Simon Rips and Michael J. Hartmann

Physik Department, Technische Universität München, James Franck Straße, 85748 Garching, Germany
(Received 19 November 2012; published 21 March 2013)

We introduce an approach to quantum information processing where the information is stored in the motional degrees of freedom of nanomechanical devices. The qubits of our approach are formed by the two lowest energy levels of mechanical resonators, which are tuned to be strongly anharmonic by suitable electrostatic fields. Single qubit rotations are conducted by radio-frequency voltage pulses that are applied to individual resonators. Two-qubit entangling gates in turn are implemented via a coupling of two qubits to a common optical resonance of a high finesse cavity. We find that gate fidelities exceeding 99% can be achieved for realistic experimental parameters.

Mechanical oscillators are among the most elementary structures that are studied in physics. Nonetheless, they have properties that make them very useful for technological applications. Their vibrational modes can, for example, undergo millions of oscillations before the motion is eventually damped and they can couple to electromagnetic fields in a very broad frequency range via their polarizability. Whereas the latter property has prompted significant effort to build optical to microwave frequency converters [1,2], the enormous Q factors of mechanical oscillators have been exploited to demonstrate approaches to mechanical computers in the classical domain [3,4]. The fascinating properties of nanomechanical oscillators furthermore motivated intense research activity towards exploring their quantum regime, which has very recently lead to breakthroughs in cooling such oscillators to their quantum ground states [5–7].

Here, we introduce an approach to quantum information processing with mechanical degrees of freedom by making use of the aforementioned exquisite properties of nanomechanical oscillators. The device we envision consists of an array of doubly clamped nanobeams that all couple to a common resonance mode of a high finesse optical cavity; see Fig. 1 for an illustration and possible setup. Each nanobeam can furthermore be manipulated individually with electrostatic and radio-frequency fields that are applied via small tip electrodes. A suitable setup for an implementation is, for example, carbon nanotubes that couple to the evanescent field of a whispering gallery mode cavity [8–14]; cf. Fig. 1.

In our scheme, the constant electric fields applied to individual nanobeams make the mechanical spectrum of each beam anharmonic and allow us to tune the respective transition frequencies. For large enough fields, the anharmonicity of the mechanical spectrum becomes comparable to the linewidth of the optical cavity resonances. By driving the cavity with a coherent input that is appropriately detuned in frequency from the closest cavity resonance, one can ensure that only one transition between eigenstates of the mechanical motion couples to the cavity. Here, we choose the laser drives such that the cavity couples to the transition between the ground and first excited state of the nanobeam. These two states, denoted $|0\rangle$ and $|1\rangle$, form our nanomechanical qubit.

As compared to previous approaches [15,16], our scheme uses the intrinsic nonlinearity of nanomechanical resonators that allows us to selectively address the qubit transitions and results in very high gate fidelities. Local operations, i.e., single qubit gates are implemented by applying suitable voltage pulses via the tip electrodes. The optical cavity mode in turn mediates interactions between any pair of mechanical qubits. If such an interaction is active for a suitable time range and combined with pertinent local operations, it can implement a fundamental entangling gate, e.g., the so-called ISWAP gate [17]. For many qubits, one can selectively apply such an ISWAP gate to any desired pair of qubits by tuning them to a transition frequency ω_G while the remaining qubits are tuned to a markedly different transition frequency ω_S via suitable voltages at the respective tip electrodes. As we show in detail below, at the end of the ISWAP gate on the selected qubits all remaining qubits can be made to return to their initial state and effectively undergo an identity operation. After successfully completing a quantum algorithm, the state of each qubit can be read out by tuning individual qubits to distinct transition frequencies and performing spectroscopy with a weak probe laser; cf. Refs. [13,14].

With all the above ingredients, the device we envision satisfies the requirements for implementing quantum computing [18]. (1) It has well-defined qubits formed by the two lowest energy eigenlevels of strongly anharmonic nanomechanical oscillators and is scalable since multiple nanobeams can couple to one high finesse optical mode. (2) It is initializable in the state $|0, 0, \ldots, 0\rangle$ by cooling the mechanical motion to the ground states, e.g., via side-band cooling [6,7]. (3) The extremely high Q factors of nanomechanical oscillators together with a cryogenic environment ensure that the coherence times of the qubits greatly
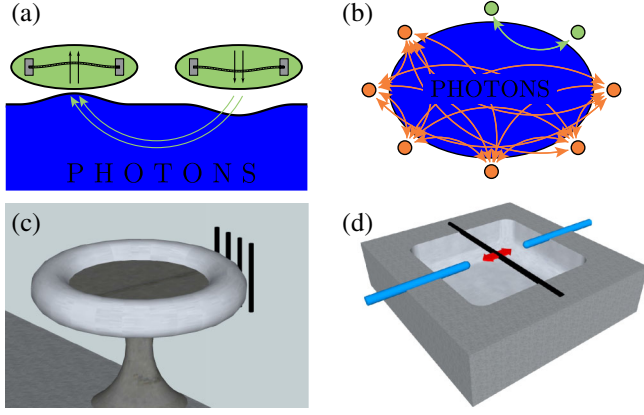
FIG. 1 (color online). Top row: Illustration of nanomechanical qubits interacting via a common photon mode: (a) The deflection of one resonator locally changes the energy density of the photon field and thus causes a force onto other resonators. (b) By properly tuning the qubit frequencies, noninteracting subsets can be defined. Bottom row: Possible implementation of the device we envision. (c) The mechanical vibration of doubly clamped carbon nanotubes couples optomechanically to the evanescent field of a whispering gallery mode in a high finesse microtoroid. (d) Electrostatic and radio-frequency fields can be applied to each nanotube (black) individually via tip electrodes (blue).

exceed gate operation times. (4) A universal set of gates can be implemented. (5) Spectroscopy on individual qubits together with single qubit rotations allows for high quantum efficiency, qubit-specific readout.

The system.—We consider a system consisting of N nanobeams that are clamped at both ends and thus feature an intrinsic nonlinearity that originates in the stretching of the material associated with its deflection [19,20]. In terms of phonon creation (annihilation) operators $b_j^\dagger$ (b_j), the Hamiltonian of one nanobeam reads

$$H_{m,j}^{(0)} = \hbar \omega_m b_j^\dagger b_j + \hbar \frac{\lambda}{2}(b_j^\dagger + b_j)^4, \qquad (1)$$

where ω_m is the resonance frequency of the harmonic motion and $\lambda = \frac{\beta}{4\hbar} x_{ZPM}^4$ is the nonlinear contribution. Here, β depends exclusively on the dimensions and material properties of the beam whereas x_{ZPM} denotes the amplitude of its zero point motion. All nanobeams are subject to static and radio-frequency electric potentials generated by tip electrodes in the close vicinity of each beam [13,14,21,22] and couple to a common optical mode of a high finesse cavity. The Hamiltonian of the entire electro-optomechanical setup in a frame that rotates at the frequency of the drive laser reads

$$H = -\hbar \Delta a^\dagger a + \sum_j \hbar g_j \left(\frac{|\alpha|}{\sqrt{2}} + X_c\right) X_j + \sum_j H_{m,j}^{(0)}$$
$$+ \sum_j [V_j^{xy}(t)X_j + V_j^z(t)X_j^2], \qquad (2)$$

where Δ is the detuning between driving laser and cavity resonance and $X_j = (b_j + b_j^\dagger)/\sqrt{2}$ is the deflection of beam j. The photon operators a and $a^\dagger$ have been shifted by their steady-state values $a \to \alpha + a$, and a negligible term $\propto a^\dagger a \sum_j X_j$ has been dropped. Hence, $X_c = (\alpha^* a + \alpha a^\dagger)/\sqrt{2}|\alpha|$ is a photon quadrature with $\alpha = \Omega/(2\Delta + i\kappa)$, where Ω is the drive amplitude of the laser and κ is the photon decay rate of the cavity.

The potentials $V_j^{xy,z}(t) = V_{j,0}^{xy,z} + V_{j,1}^{xy,z}(t)$ describe constant $V_{j,0}^{xy,z}$ and time-dependent $V_{j,1}^{xy,z}(t)$ gradient forces caused by the voltages applied to the tip electrodes. The constant parts tune the equilibrium positions of the mechanical oscillators via $V_{j,0}^{xy}$ and their spectrum via $V_{j,0}^z$, whereas the time-dependent parts $V_{j,1}^{xy}(t)$ can implement single qubit rotations. We always choose $V_{j,0}^{xy} = -\hbar g_j \frac{|\alpha|}{\sqrt{2}}$ such that the nanobeams remain undeflected. $g_j = 2|\alpha|x_{ZPM,j}G_0$ is the optomechanical coupling that can be controlled by the amplitude of the laser drive, where $G_0 = \partial\omega/\partial X$ is the cavity's frequency shift per resonator deflection. We use the radio-frequency fields $V_{j,1}(t)$ and the couplings g_j as controls to perform gate operations.

In a realistic experimental situation, the mechanical motion will be subject to damping at a rate γ_m and cavity photons will be lost at a rate κ. The full dynamics of our system that takes these incoherent processes into account can thus be described by the master equation

$$\dot\varrho = -i[H, \varrho] + \frac{\gamma_m}{2}\sum_j [\bar n \mathcal{D}_{\uparrow,j}(b_j) + (\bar n + 1)\mathcal{D}_{\downarrow,j}(b_j)]$$
$$+ \frac{\kappa}{2}\mathcal{D}_{\downarrow,c}(a), \qquad (3)$$

where $\bar n$ is the thermal phonon number at the environment temperature T and the dissipators read $\mathcal{D}_{\downarrow}(y) = 2y\varrho y^\dagger - y^\dagger y\varrho - \varrho y^\dagger y$ and $\mathcal{D}_{\uparrow}(y) = 2y^\dagger \varrho y - yy^\dagger\varrho - \varrho yy^\dagger$.

Nanomechanical qubits.—The qubits we consider are formed by the two lowest energy levels of our nanomechanical beams. Mechanical resonators feature a small intrinsic anharmonicity in any deflection mode that can be enhanced by electrostatic gradient forces; see Refs. [13,14] for details. Suitably tuned electrostatic fields generate an inverted harmonic potential of the form $V \propto -X^2$ that counteracts the harmonic part of the elastic restoring force. The electrostatic potential thus softens the mechanical resonance mode and hence reduces its frequency. Since the deflection per phonon x_{ZPM} is proportional to $\omega_m^{-1/2}$, a reduction of ω_m causes a significant enhancement of the nonlinearity as $\lambda \propto x_{ZPM}^4 \propto \omega_m^{-2}$; cf. Refs. [13,14].

It is useful to consider a "tuned" mechanical Hamiltonian $H_{m,j} = H_{m,j}^{(0)} + \sum_j V_{j,0}^z X_j^2$ that includes the constant parts of the V_j^z. We write $H_{m,j}$ and the deflection X_j of each mechanical resonator in the eigenbasis of $H_{m,j}$; i.e., $H_{m,j} = \sum_n E_{n,j}|n\rangle_j\langle n|_j$ and $X_j = \sum_{nm} X_{nm,j}|n\rangle_j\langle m|_j$, where
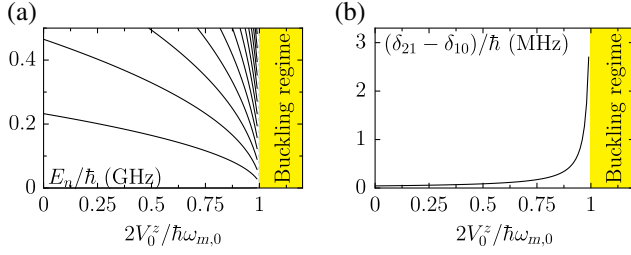
FIG. 2 (color online). (a) Nonlinear phonon spectrum of a nanobeam in the presence of a softening field V_0^z. For $2V_0^z > \hbar\omega_{m,0}$, the beam enters the bistable buckling regime. (b) Effective nonlinearity of the phonon spectrum $\delta_{21} - \delta_{10}$. A sufficiently high value of $\delta_{21} - \delta_{10}$ suppresses unwanted processes of the type $|11\ldots\rangle \to |20\ldots\rangle$.

$H_{m,j}|n\rangle_j = E_{n,j}|n\rangle_j$. The $E_{n,j}$ and $X_{nm,j}$ can be found numerically; see Fig. 2(a).

Provided the nonlinearity per phonon is large enough and the mechanical motion is cooled to the ground state, we can restrict our analysis to the two lowest energy levels $|0\rangle_j$ and $|1\rangle_j$ of each resonator, which form our qubits. The nonlinearity of the qubits, i.e., the fact that the qubit transition energies $\hbar\delta_{10,j} = E_{1,j} - E_{0,j}$ differ significantly from transition energies between higher states $\hbar\delta_{nm,j} = E_{n,j} - E_{m,j}$, especially from $\hbar\delta_{21,j}$ [see Fig. 2(b)], ensures that the restriction to these two levels remains a very accurate approximation throughout the gate sequences. To explain the gate operations in detail we now switch to an interaction picture with respect to $H_0 = -\hbar\Delta a^\dagger a + \sum_j H_{m,j}$.

Local operations and single qubit gates.—Local operations, that is, rotations about the σ_x, σ_y, and σ_z axes, are realized by applying time-dependent gradient forces as encoded in the potentials $V_j^{xy}(t)$ and $V_j^z(t)$ in Eq. (2).

We obtain σ_z rotations by temporarily shifting the qubit transition frequency δ_{10}, which makes the qubit rotate at a different rate and hence collect a phase shift. This is achieved by tuning the softening fields that control the mechanical frequency to a different value for a suitable time which adds a term $V^z X^2$ to the Hamiltonian that shifts the qubit frequency $\delta_{10} \to \delta_{10} + \delta_{10}^{(1)}(t)$ (we skip the qubit index j throughout the discussion of local operations). For $\int \delta_{10}^{(1)} dt = \phi/2$, this procedure implements the operation

$$e^{-i\int V^z(t)X^2 dt/\hbar} \approx e^{-i\sigma_z\phi/2} \equiv -[\phi]_{\bar{z}}. \tag{4}$$

The σ_x and σ_y rotations can be implemented by applying gradient forces related to V^{xy}. If the potential $V^{xy}(t)$ is a pulse that is modulated by an oscillation at the qubit frequency $V^{xy}(t) = \cos(\delta_{10}t + \theta)\tilde{V}^{xy}$, one finds $\tilde{V}^{xy}\cos(\delta_{10}t+\theta)e^{iH_0t/\hbar}Xe^{-iH_0t/\hbar} \approx \tilde{V}^{xy} \times \frac{X_{01}}{2}[\cos(\theta)(\sigma^{01}+\sigma^{10}) + i\sin(\theta)(\sigma^{01} - \sigma^{10})]$, where $\sigma^{ab} = |a\rangle\langle b|$ and we have dropped off-resonant contributions. Thus, for $\theta = 0$ and $\int dt\tilde{V}^{xy}(t) = \phi/X_{01}$, one finds

$$e^{-i\int dtV^{xy}(t)X} \approx e^{-i\sigma_x\phi/2} \equiv -[\phi]_{\bar{x}}, \tag{5}$$

and for $\theta = \pi/2$ and $\int dt\tilde{V}_{xy}(t) = \phi/X_{01}$

$$e^{-i\int dtV^{xy}(t)X} \approx e^{-i\sigma_y\phi/2} \equiv -[\phi]_{\bar{y}}. \tag{6}$$

Effective interactions and two-qubit gates.—In order to implement entangling two-qubit operations, we employ an indirect interaction between mechanical resonators that is mediated by an optical cavity mode [23]. Here, the laser is sufficiently far detuned from any resonance, such that $g_j \ll |\Delta \pm \delta_{nm,j}|$. For an initial state in the qubit subspace formed by $|0\rangle_j$ and $|1\rangle_j$, this condition ensures that the dynamics is restricted to this subspace. To perform a gate operation on two qubits, e.g., with indices $j = \{1, 2\}$ ("gate qubits"), we tune those two qubits to a common transition frequency ω_G and hence common coupling g_G, while tuning the remaining qubits ("saved qubits") to a sufficiently different transition frequency ω_S and coupling g_S such that $|\omega_G - \omega_S| \gg g_G, g_S$ and interactions between gate qubits and saved qubits are strongly suppressed. To explain the working principle of this gate, we consider a scenario where $V_{j,1}^{xy,z} = 0$. An adiabatic elimination of the photons together with a rotating wave approximation yields the effective Hamiltonian

$$H_{eff} \approx H_G + H_S,$$

$$H_G = \hbar\frac{g_G^2\Delta X_G^2}{\Delta^2 - \omega_G^2}(\sigma_1^{01}\sigma_2^{10} + \text{H.c.}) + \sum_{j=1}^{2} H_{G,j},$$

$$H_S = \hbar\frac{g_S^2\Delta X_S^2}{\Delta^2 - \omega_S^2}\sum_{i \neq j > 2}(\sigma_i^{01}\sigma_j^{10} + \text{H.c.}) + \sum_{j>2} H_{S,j}, \tag{7}$$

where $H_{G/S,j} = \hbar\frac{g_j^2}{2}(c_{G/S}^0\sigma_j^{00} + c_{G/S}^1\sigma_j^{11})$ and $\sigma_j^{ab} = |a\rangle\langle b|_j$. Here, $X_{G/S}$ denotes the displacement matrix element $X_{01,j}$ and $c_{G/S}^n = \sum_m(X_{nm,j}^2)/(\Delta + \delta_{nm,j})$ are the interaction-induced energy shifts for the gate qubits ($j = 1, 2$) and saved qubits ($j > 2$), respectively; see Supplemental Material [24]. The corresponding phase shifts can be reversed after the gate operation by appending a suitable σ_z rotation.

The time evolution of the Hamiltonian (7) can be used to perform an ISWAP operation on distinct gate qubits, while the other qubits are unaffected. This can be achieved by decomposing the ISWAP operation into $\sqrt{\pm\text{ISWAP}}$ operations, using the identity

$$\boxed{\sqrt{\text{ISWAP}}}-[\pi]_{\bar{z}}\boxed{\sqrt{-\text{ISWAP}}}-[-\pi]_{\bar{z}} = \boxed{\text{ISWAP}} \tag{8}$$

Here, the $\sqrt{\pm\text{ISWAP}}$ operations are implemented by choosing laser drive pulses such that $(\Delta X_G^2)/(\Delta^2 - \omega_G^2) \times \int g_G(t)^2 dt = \pm\frac{\pi}{4}$, respectively. The $\sqrt{\text{ISWAP}}$ and the $\sqrt{-\text{ISWAP}}$ operations thus only differ by the sign of the employed detuning Δ. During the $\sqrt{\text{ISWAP}}$ operation on the gate qubits, the saved qubits are subject to the dynamics

generated by H_S [compare to Fig. 1(b)]. Yet since there are no local $-[\pi]_{\bar{z}}$ operations on the saved qubits, this evolution is reversed during the subsequent $\sqrt{-\text{ISWAP}}$ operation on the gate qubits and the saved qubits return back to their initial states.

Numerical results.—We analyzed the fidelities of the quantum gates we propose by numerically solving Eq. (3) involving two and four qubits, where we included the lowest three levels $|0\rangle$, $|1\rangle$, $|2\rangle$ for each resonator (qubit). To find an estimate for the fidelity of the gate operations, we compute the fidelity $f(\sigma, \rho) = \text{Tr}(\sqrt{\sqrt{\rho}\sigma\sqrt{\rho}})$ of the desired target state σ with the actual state ρ that results from the full dynamical evolution for several initial states. In order to confirm that relative phases of the states evolve as desired, we use all states of the form $|\phi\rangle = (|j, k, \ldots\rangle + |0, 0, \ldots\rangle)/\sqrt{2}$ $(j, k, \ldots = 0, 1)$ as initial states and average the fidelity f over these, $F = \overline{f(\sigma, \rho)}|_{\text{all } |\phi\rangle}$. Figure 3 shows the resulting gate error $\mathcal{E} = 1 - F$ as a function of the gate time T_G, the laser detuning Δ, and the mechanical and optical dissipation rates γ_m and κ. To demonstrate the scalability of our approach, we present results for two qubits (solid lines) as well as for four qubits (red dots). For the four-qubit case, the gate is applied to two qubits while the remaining two return to their initial state. These results clearly show the excellent scaling properties of our approach.

The results given in Fig. 3 are found for (10,0)-carbon nanotubes of length $L = 300$ nm and radius $R = 0.39$ nm, coupled to the evanescent field of a microtoroid cavity;
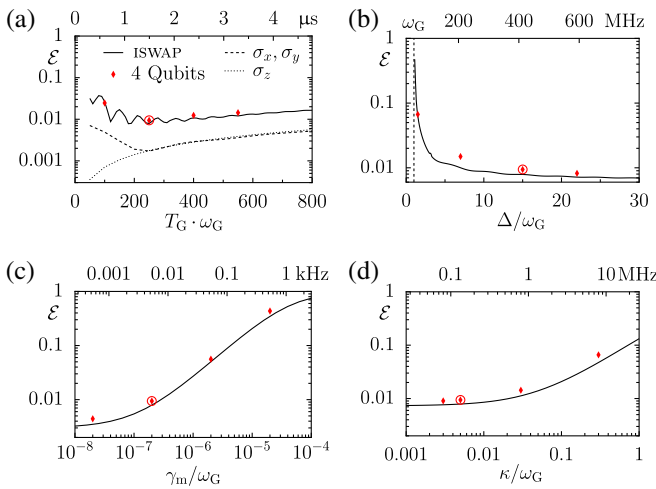

FIG. 3 (color online). Error $\mathcal{E} = 1 - F$ of gate operations. Except for the quantities on the horizontal axes, all parameters are as in the setting described in the main text. Solid lines show results for two qubits, and red dots show results for four qubits. Highlighted red dots correspond to the parameter example discussed in the text. (a) Error as a function of the gate time for local and entangling operations. Note that changing the gate time also changes the required coupling rate. (b) Error as a function of the laser detuning. [(c) and (d)] Illustration of the influence of damping for the photons and resonators, respectively.

see Refs. [13,14] for details. By softening the mechanical resonance frequency of the gate qubits down to $\omega_G/2\pi = 26.6$ MHz, we achieve a nonlinearity of $(\delta_{21} - \delta_{10})/2\pi = 2.71$ MHz. The optomechanical coupling of carbon nanotubes can be dramatically enhanced by employing a cavity resonance in the vicinity of recently demonstrated excitonic resonances [24–26]. We choose a cavity frequency that is far enough from such a resonance to sufficiently suppress additional absorption and estimate that an optomechanical coupling rate of $g_G/2\pi = 8.73$ MHz can be achieved with a laser drive of 5.30 W input power that is detuned by $\Delta/2\pi = 0.399$ GHz from the cavity frequency. For a gate time of $T_G = 1.49$ μs, such coupling suffices for the $\sqrt{\text{ISWAP}}$ operation assuming a rectangular pulse. Furthermore, we assume an ambient temperature of 20 mK, a mechanical Q factor of 5×10^6 for the tuned resonator [10], and a total photon decay rate (including intrinsic cavity losses and losses induced by the exciton resonance) of $\kappa/2\pi = 133$ kHz [27,28]. Note that for our conditions with $\kappa^2/\Delta^2 = 8 \times 10^{-8}$ this corresponds to an absorbed power of ~ 18 nW that is comfortably compatible with a cryogenic environment [29]. Moreover, even higher finesses and lower absorption could be attained in crystalline resonators [30]. For tuning the mechanical resonances, electrostatic fields of 76 V/μm are required, whereas for the local operations $\sigma_{x,y}[\phi]$, we find radiofrequency field amplitudes of ~ 1 V/μm, depending on operation time and angle ϕ. For the static fields that compensate the photon-induced shift of the equilibrium position during an entangling operation, 6.1 V/μm is needed and the $\sigma_z[\phi]$ operations require a gate time $>\phi/\omega_G$ to avoid buckling the resonator. Importantly, decoherence due to electric noise in the electrodes, such as Johnson-Nyquist or $1/f$ noise, is in our setup negligible compared to the mechanical damping $\gamma_m \bar{n}$ [24].

Conclusions.—In summary, we have introduced an approach to quantum information processing with nanomechanical qubits. Our approach is realizable with current or near-future experimental technology. Importantly, the nanomechanical resonators in our approach show very promising scalability properties and are not vulnerable to fluctuations of background charges such as superconducting qubits. The performance of our scheme could be improved further with optimized laser and radio-frequency control pulses. Alternative platforms for implementation could consist of stiff nanobeams with high optomechanical couplings such as photonic crystal nanobeam cavities in diamond [31]. For building even larger scale devices, our scheme could also be integrated into optomechanical networks of multiple cavities [32].

[1] Sh. Barzanjeh, M. Abdi, G. J. Milburn, P. Tombesi, and D. Vitali, Phys. Rev. Lett. **109,** 130503 (2012).

[2] C. A. Regal and K. W. Lehnert, J. Phys. Conf. Ser. **264,** 012025 (2011).

[3] S. C. Masmanidis, R. B. Karabalin, I. De Vlaminck, G. Borghs, M. R. Freeman, and M. L. Roukes, Science **317,** 780 (2007).

[4] I. Mahboob, E. Flurin, K. Nishiguchi, A. Fujiwara, and H. Yamaguchi, Nat. Commun. **2,** 198 (2011).

[5] A. D. O'Connell, M. Hofheinz, M. Ansmann, R. C. Bialczak, M. Lenander, E. Lucero, M. Neeley, D. Sank, H. Wang, M. Weides, J. Wenner, J. M. Martinis, and A. N. Cleland, Nature (London) **464,** 697 (2010).

[6] J. D. Teufel, T. Donner, Dale Li, J. H. Harlow, M. S. Allman, K. Cicak, A. J. Sirois, J. D. Whittaker, K. W. Lehnert, and R. W. Simmonds, Nature (London) **475,** 359 (2011).

[7] J. Chan, T. P. Mayer Alegre, A. H. Safavi-Naeini, J. T. Hill, A. Krause, S. Gröblacher, M. Aspelmeyer, and O. Painter, Nature (London) **478,** 89 (2011).

[8] G. A. Steele, A. K. Hüttel, B. Witkamp, M. Poot, H. B. Meerwaldt, L. P. Kouwenhoven, and H. S. J. van der Zant, Science **325,** 1103 (2009).

[9] B. Lassagne, Y. Tarakanov, J. Kinaret, D. Garcia-Sanchez, and A. Bachtold, Science **325,** 1107 (2009).

[10] A. K. Hüttel, G. A. Steele, B. Witkamp, M. Poot, L. P. Kouwenhoven, and H. S. J. van der Zant, Nano Lett. **9,** 2547 (2009).

[11] G. Anetsberger, O. Arcizet, Q. P. Unterreithmeier, R. Riviére, A. Schliesser, E. M. Weig, J. P. Kotthaus, and T. J. Kippenberg, Nat. Phys. **5,** 909 (2009).

[12] G. Anetsberger, E. Gavartin, O. Arcizet, Q. P. Unterreithmeier, E. M. Weig, M. L. Gorodetsky, J. P. Kotthaus, and T. J. Kippenberg, Phys. Rev. A **82,** 061804 (2010).

[13] S. Rips, M. Kiffner, I. Wilson-Rae, and M. J. Hartmann, New J. Phys. **14,** 023042 (2012).

[14] S. Rips, I. Wilson-Rae, and M. J. Hartmann, arXiv:1206.0147.

[15] K. Stannigel, P. Komar, S. J. M. Habraken, S. D. Bennett, M. D. Lukin, P. Zoller, and P. Rabl, Phys. Rev. Lett. **109,** 013603 (2012).

[16] M. Schmidt, M. Ludwig, and F. Marquardt, New J. Phys. **14,** 125005 (2012).

[17] N. Schuch and J. Siewert, Phys. Rev. A **67,** 032301 (2003).

[18] D. P. DiVincenzo, Fortschr. Phys. **48,** 771 (2000).

[19] S. M. Carr, W. E. Lawrence, and M. N. Wybourne, Phys. Rev. B **64,** 220101 (2001).

[20] P. Werner and W. Zwerger, Europhys. Lett. **65,** 158 (2004).

[21] C. C. Wu and Z. Zhong, Nano Lett. **11,** 1448 (2011).

[22] K. H. Lee, T. G. McRae, G. I. Harris, J. Knittel, and W. P. Bowen, Phys. Rev. Lett. **104,** 123604 (2010).

[23] M. J. Hartmann and M. B. Plenio, Phys. Rev. Lett. **101,** 200503 (2008).

[24] See Supplemental Material at http://link.aps.org/supplemental/10.1103/PhysRevLett.110.120503 for details.

[25] M. S. Hofmann, J. T. Glückert, and A. Högele, arXiv:1209.3429v1.

[26] I. Wilson-Rae, C. Galland, W. Zwerger, and A. Imamoğlu, New J. Phys. **14,** 115003 (2012).

[27] T. J. Kippenberg, S. M. Spillane, and K. J. Vahala, Appl. Phys. Lett. **85,** 6113 (2004).

[28] M. Pöllinger, D. O'Shea, F. Warken, and A. Rauschenbeutel, Phys. Rev. Lett. **103,** 053901 (2009).

[29] R. Riviére, S. Deléglise, S. Weis, E. Gavartin, O. Arcizet, A. Schliesser, and T. J. Kippenberg, Phys. Rev. A **83,** 063835 (2011).

[30] J. Hofer, A. Schliesser, and T. J. Kippenberg, Phys. Rev. A **82,** 031804(R) (2010).

[31] B. M. Hausmann, J. T. Choy, T. M. Babinec, B. J. Shields, I. Bulu, M. D. Lukin, and M. Lončar, Phys. Status Solidi A **209,** 1619 (2012).

[32] K. Stannigel, P. Rabl, A. S. Sørensen, P. Zoller, and M. D. Lukin, Phys. Rev. Lett. **105,** 220501 (2010).